

Photoeffects in Undoped and Doped SrTiO₃ Ceramic Electrodes

KI HYUN YOON AND TAE HEUI KIM

Department of Ceramic Engineering, Yonsei University, Seoul, Korea

Received April 1, 1986; in revised form August 12, 1986

Photoeffects in SrTiO₃ ceramic anodes, undoped and Nb₂O₅, Sb₂O₃, and V₂O₅ doped, have been investigated. Photoresponses in undoped SrTiO₃ electrodes appear at a wavelength of about 390 nm and the quantum efficiency is about 3.5% at a wavelength of 340 nm for a bias of 0.5 V vs Ag/AgCl. Photocurrents of Nb₂O₅-, Sb₂O₃-, and V₂O₅-doped SrTiO₃ electrodes decrease as the amount of dopant increases. The onset of photocurrent for both Nb₂O₅- and Sb₂O₃-doped electrodes is at 390 nm while for the V₂O₅-doped electrode it is at 500 nm. © 1987 Academic Press, Inc.

Introduction

As hydrogen is a nonpolluting fuel which can be easily used and is highly energy intensive, many researchers have been interested in its production (1). Among many production methods, photoelectrochemical conversion using sunlight and water is said to be relatively more economical.

Fujishima and Honda have suggested that it is possible to dissolve water into hydrogen and oxygen by photoelectrochemical conversion using a single crystal TiO₂ electrode (2). But even though the energy band gap of SrTiO₃ (~3.2 eV) is larger than that of TiO₂ (~3.0 eV), SrTiO₃ photoelectrodes have shown higher conversion efficiency because of the lower electron affinity (3, 4). Only radiation with wavelengths shorter than 390 nm is effective with SrTiO₃ electrodes. If the photoresponse region could be expanded, SrTiO₃ would become a very excellent material for photoelectrochemical conversion.

In this experiment we used SrTiO₃ ceramic electrodes, which are easy to prepare and to which additives may be added quantitatively, and observed their photoelectrochemical characteristics and the influence of additives, Nb₂O₅, Sb₂O₃, and V₂O₅.

Experimental

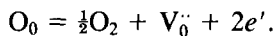
The starting material was SrTiO₃ powder having a purity of 99.9% and the additives Nb₂O₅, Sb₂O₃, and V₂O₅ were powders having purities of 99.9%. Additives were added in portions of 0 to 1.0 mol%. Each mixed powder was isostatically pressed under a pressure of 20,000 psi into a pellet with a diameter of 14 mm and a thickness of 4 mm. They were sintered in hydrogen at 1350°C for 4 hr. The sinters were sliced and polished with SiC abrasive papers to a thickness of 0.2 mm. These specimens had copper wires attached by silver paste and were sealed over with epoxy resin except on the face to be illuminated to prevent contact

with the electrolyte. Current-voltage curves for the SrTiO₃-silver paste electrode junction were found to follow Ohm's law.

The PEC cell is the same as that used in experiments with polycrystalline TiO₂ electrodes which have been reported on from this laboratory (5-7). The apparatus for measurement of the characteristics is also the same as that used in experiments on polycrystalline TiO₂ electrodes (6, 7). With this equipment the photocurrent-voltage and photocurrent-wavelength characteristics and quantum efficiency were measured.

Results and Discussion

When singly crystal SrTiO₃ is reduced by hydrogen, oxygen vacancies are formed and electrons released for charge compensation,



SrTiO₃ is dark gray and is an *n*-type semiconductor due to the oxygen vacancies (3, 9, 10). As the SrTiO₃ ceramic electrode sintered in hydrogen also turns dark gray, it can be seen to be an *n*-type semiconductor.

The wavelength at which the photoresponse in the pure SrTiO₃ ceramic electrode begins to appear is 390 nm, which is nearly equivalent to the energy band gap of SrTiO₃ (~3.2 eV) (12) and is consistent with that reported for single crystal SrTiO₃ electrodes (3, 10, 11). These suggest that the mobility of the electric carriers and the photoabsorptivity of the polycrystalline SrTiO₃ structure of the sinters do not differ much from those of a single crystal.

When the additives, Nb₂O₅, Sb₂O₃, and V₂O₅ are added to SrTiO₃, the defect equations

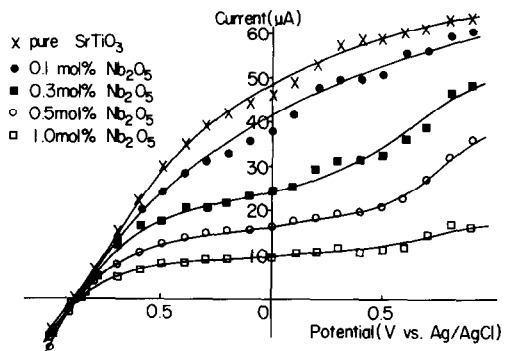
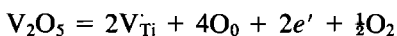
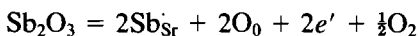
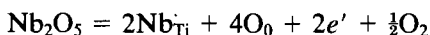


FIG. 1. *I*-*V* curves for SrTiO₃ ceramic electrodes doped with Nb₂O₅.

can be formed (8). Therefore it was expected that the increased electrical conductivity of the specimens would increase the photocurrents. But as shown in Figs. 1-3, the photocurrent decreased as the amount of additive increased. Kennedy *et al.* (14), in an experiment on the α-Fe₂O₃ electrode with SnO₂, observed similar results. According to the report by Butler (13), the photocurrent is given by

$$J = q\psi_0 \left\{ 1 - \frac{\exp(-\alpha w)}{1 + L_p} \right\}$$

and the depletion layer width is given by

$$w = \left(\frac{2\epsilon_0}{qN_d} \right)^{1/2} (V - V_{fb})$$

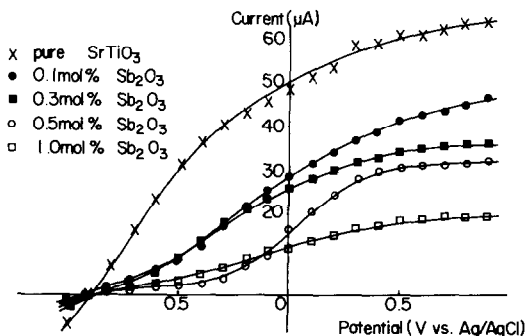


FIG. 2. *I*-*V* curves for SrTiO₃ ceramic electrodes doped with Sb₂O₃.

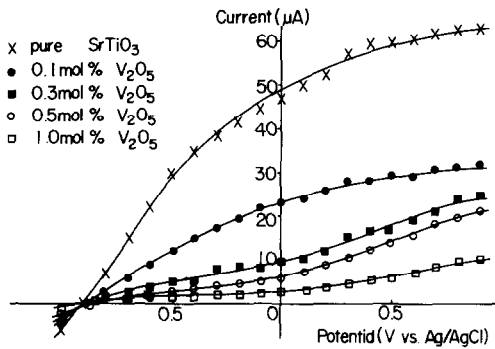


FIG. 3. I - V curves for SrTiO₃ ceramic electrodes doped with V₂O₅.

where ψ_0 is the photon flux, L_p the hole diffusion length, V_{fb} the flatband potential, and N_d is the donor density. From these equations, as the amount of additive is increased the donor density increases, and the depletion layer width decreases. Consequently the photocurrent decreases. It seems that the decrease in depletion layer width contributes more than the increase in electrical conductivity does. In Fig. 3, the extent of decrease in the photocurrent is larger than those in Figs. 1 and 2. Harten (15) reported that the energy level in the band gap acts as a recombination center facilitating electron-hole recombination. According to the report by Matsumoto *et al.* (16), when Co

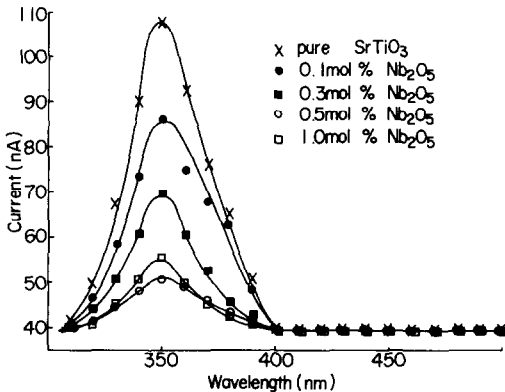


FIG. 4. I - λ curves for SrTiO₃ ceramic electrodes doped with Nb₂O₅.

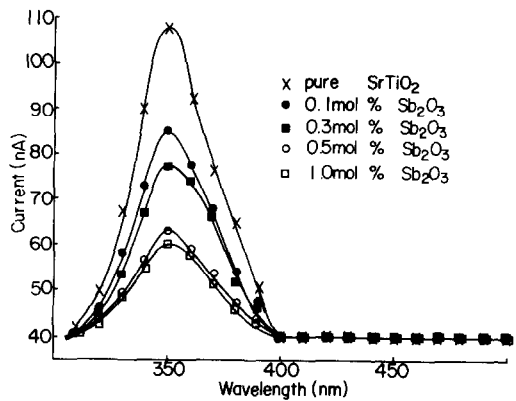


FIG. 5. I - λ curves for SrTiO₃ ceramic electrodes doped with Sb₂O₃.

was added to TiO₂, the formation of an intermediate level was attributed to the interaction of d orbitals. And Monnier and Augustinski (17) reported that for TiO₂ the addition of Ni, Cr, and Zn decreases the photocurrent because the intermediate level plays the role of a recombination center. Therefore, it is assumed that in this case also the reason for the larger decrease is the intermediate level acting as a recombination center, as well as the decrease of the depletion layer width.

Figures 4 and 5 are the photocurrent-wavelength characteristics of SrTiO₃ ceramic electrodes with Nb₂O₅ and Sb₂O₃, respectively. As shown, the wavelength of the light at which photoresponse starts is equal to that in the undoped SrTiO₃ ceramic electrode. This means that the addition of Nb₂O₅ or Sb₂O₃ does not influence the band gap of SrTiO₃, for interaction of d orbitals cannot occur because the $4d$ orbit in Nb is empty and in Sb the d orbit is occupied (18). In Fig. 6, the photocurrent-wavelength characteristics of SrTiO₃ ceramic electrodes with V₂O₅, it is seen that the wavelength of light at which the photoresponse appears shifted to about 500 nm, longer than the 390 nm for the undoped SrTiO₃ ceramic electrode. Matsumoto *et al.* (16)

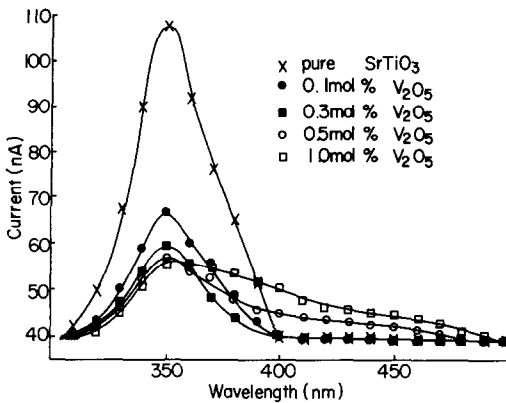


FIG. 6. I - λ curves for SrTiO_3 ceramic electrodes doped with V_2O_5 .

reported that when Co was added to TiO_2 , the photoresponse started at a longer wavelength due to the intermediate level formed by interaction of d orbitals. Monnier and Augustinski (17) and Ghosh and Maruska (20) reported that visible light response appeared due to the formation of intermediate levels in the band gap, which can originate from impurity cations or/and from defects induced by doping Cr, Ni, and Zn in TiO_2 . Odekirk and Blakemore in an experiment on the SrTiO_3 electrode with La also reported that visible light response was due to the formation of impurity bands (21). Campet *et al.* reported that d energy levels of V were localized within the optical band of TiO_2 (22). Therefore, comparing with the conduction and valence band levels of various electrode materials (23), it can be expected that $3d$ energy levels of V lie within the band gap of SrTiO_3 . In the case of SrTiO_3 electrodes with Cr, etc., Matsumura *et al.* (19) observed similar results. When V_2O_5 is added to SrTiO_3 , the $3d$ orbitals of Ti and V interact to form an intermediate level. And for electrons excited through this intermediate level, the photoresponse starts at a longer wavelength which has the lower energy.

The quantum efficiency, η , is the number

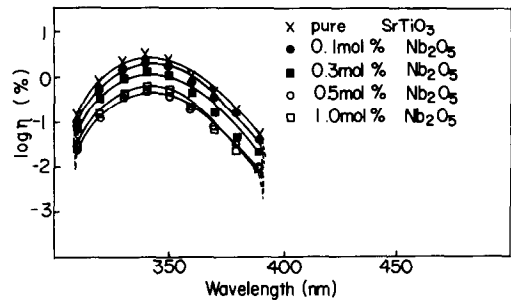


FIG. 7. Quantum efficiencies for SrTiO_3 ceramic electrodes doped with Nb_2O_5 .

of electrons in the circuit per incident photon and is given by

$$\eta = \frac{J_e/e}{W_\lambda/h\nu}$$

where J_e is the current density (A/cm^2), W_λ is the energy of the incident photon (W/cm^2), h is Planck's constant ($6.63 \times 10^{-34} \text{ J} \cdot \text{sec}$), ν is determined by C_0/λ , and C_0 is the speed of light in vacuum ($3.0 \times 10^{10} \text{ cm}/\text{sec}$). The quantum efficiencies from this equation are shown in Figs. 7-9. In the undoped SrTiO_3 ceramic electrode, the quantum efficiency is about 3.5% ($V_{\text{app}} = 0.5 \text{ V}$ vs Ag/AgCl) at a wavelength of 340 nm. And in the case of electrodes with V_2O_5 , it is seen that light in the visible region, where much more radiation is available, can be effective.

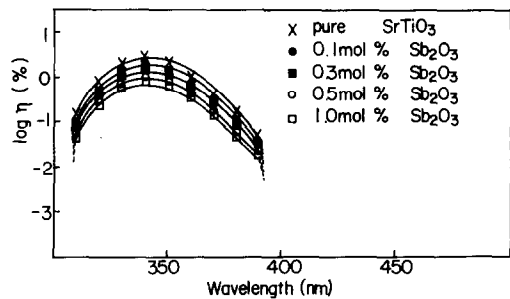


FIG. 8. Quantum efficiencies for SrTiO_3 ceramic electrodes doped with Sb_2O_3 .

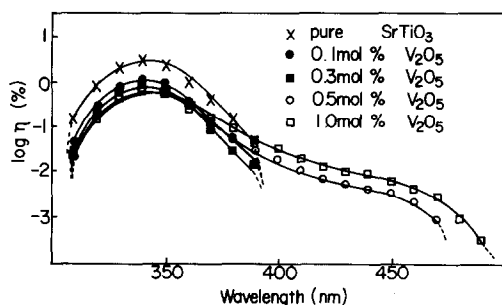


FIG. 9. Quantum efficiencies for SrTiO₃ ceramic electrodes doped with V₂O₅.

Conclusion

In the undoped SrTiO₃ ceramic electrode, the wavelength at which photoreponse appears was equivalent to that for a single crystal SrTiO₃ electrode. And the quantum efficiency was about 3.5% ($V_{app} = 0.5$ V vs Ag/AgCl) at 340 nm.

In the electrodes with Nb₂O₅ or Sb₂O₃, the photocurrent decreased as the amount of additive increased, and the photoreponse started at a wavelength of 390 nm. In the electrodes with V₂O₅, the photocurrent decreased as the amount of V₂O₅ increased, but the wavelength for photoreponse appeared shifted to 500 nm.

References

1. G. G. LIBOWITZ, "Hydrides for Energy Storage," p. 1, Pergamon, Norway (1977).
2. A. FUJISHIMA AND K. HONDA, *Nature (London)* **238**, 37 (1972).
3. J. G. MAVROIDES, J. A. KAFALAS, AND D. F. KOLEGAR, *Appl. Phys. Lett.* **28**, 241 (1976).
4. M. A. BUTLER AND D. S. GINLEY, *J. Electrochem. Soc.* **125**, 22 (1978).
5. K. H. YOON AND S. O. YOON, *Japan J. Appl. Phys.* **23**, 113 (1984).
6. K. H. YOON, J. S. KIM, AND S. O. YOON, *J. Kor. Ceram. Soc.* **20**, 356 (1983).
7. K. H. YOON AND D. H. KANG, *I & EC Prod. Res. & Dev.* **25**, 93 (1986).
8. N. H. CHAN, R. K. SHARMA, AND D. M. SMYTH, *J. Electrochem. Soc.* **128**, 1762 (1981).
9. L. C. WALTERS AND R. E. GRACE, *J. Phys. Chem.* **28**, 239 (1967).
10. M. S. WRIGHTON, A. B. ELLIS, P. T. WOLCZANSKI, D. L. MORSE, H. B. ABRAHAMSON, AND D. S. GINLEY, *J. Amer. Chem. Soc.* **98**, 1774 (1976).
11. T. WATANABE, A. FUJISHIMA, AND K. HONDA, *Bull. Chem. Soc. Japan* **49**, 355 (1976).
12. J. M. BOLTS AND M. S. WRIGHTON, *J. Phys. Chem.* **80**, 2641 (1976).
13. M. A. BUTLER, *J. Appl. Phys.* **48**, 1914 (1977).
14. J. H. KENNEDY, M. ANDERMAN, AND R. SHINAR, *J. Electrochem. Soc.* **128**, 2371 (1981).
15. H. U. HARTEN, *Electrochim. Acta* **13**, 1255 (1968).
16. Y. MATSUMOTO, J. KURIMOTO, Y. AMAGASAKI, AND E. SATO, *J. Electrochem. Soc.* **127**, 2148 (1980).
17. A. MONNIER AND J. AUGUSTINSKI, *J. Electrochem. Soc.* **127**, 1576 (1980).
18. R. C. EVANS, "An Introduction to Crystal Chemistry", 2nd ed., p. 21, Cambridge Univ. Press, London/New York (1964).
19. M. MATSUMURA, M. HIRAMOTO, AND H. TSUBOMURA, *J. Electrochem. Soc.* **130**, 326 (1983).
20. A. K. GHOSH AND H. P. MARUSKA, *J. Electrochem. Soc.* **124**, 1516 (1977).
21. B. ODEKIRK AND J. S. BLAKEMORE, *J. Electrochem. Soc.* **130**, 321 (1983).
22. G. CAMPET, J. VERNIOLLE, J. P. DOUMERC, AND J. CLAVERIE, *Mat. Res. Bull.* **15**, 1135 (1980).
23. H. H. KUNG, H. S. JARRETT, A. W. SLEIGHT, AND A. FERRETTI, *J. Appl. Phys.* **48**, 2463 (1977).